Effect of Step Stiffness and Diffusion Anisotropy on the Meandering of a Growing Vicinal Surface

Thomas Frisch, Alberto Verga

Effect of step stiffness and diffusion anisotropy on the meandering of a growing vicinal surface

Thomas Frisch* and Alberto Verga†
Institut de Recherche sur les Phénomènes Hors Équilibre, UMR 6594, CNRS, Université de Provence, Marseille, France
(Dated: April 11, 2006)

We study the step meandering instability on a surface characterized by the alternation of terraces with different properties, as in the case of Si(001). The interplay between diffusion anisotropy and step stiffness induces a finite wavelength instability corresponding to a meandering mode. The instability sets in beyond a threshold value which depends on the relative magnitudes of the destabilizing flux and the stabilizing stiffness difference. The meander dynamics is governed by the conserved Kuramoto-Sivashinsky equation, which display spatiotemporal coarsening.

PACS numbers: 81.15.Hi, 68.35.Ct, 81.10.Aj, 47.20.Hw

Molecular beam epitaxy (MBE) is often used to grow nanostructures on vicinal surfaces of semiconductor and metallic crystals [1–5]. Under nonequilibrium growth a very rich variety of crystal surface morphologies are experimentally observed resulting from the nonlinear evolution of step bunching and meandering instabilities [6–8]. Self-organized patterns arising from these instabilities may be used for the development of technological applications such as quantum dots and quantum wells [9, 10]. The step meandering instability was originally predicted theoretically by Bales and Zangwill [11] for a vicinal surface under growth. Its origin comes from the asymmetry between the descending and ascending currents of adatoms. Nonlinear extensions of this work have shown that the meander evolution can be described by amplitude equations showing diverse behaviors: spatiotemporal chaos governed by the Kuramoto-Sivashinsky equation in the case of the Erlich-Schwoebel effect with desorption [12]; nonlinear coarsening in the case of negligible desorption [13–15]; and interrupted coarsening when two-dimensional anisotropy is included [16, 17]. Step meandering on a Si(001) vicinal surface can also be driven by a drift electromigration current in the presence of alternating diffusion coefficients, even for symmetric adatom attachment to the steps [18, 19].

Recent experiments [20–23] on the growth of Si(001) have revealed the existence of a step bunching instability and the development of a transverse two-dimensional complex structure (ripples), possibly reminiscent of a meandering instability. We have recently shown that the observed step bunching instability is due to the interplay between the elastic interactions and the alternation of the step parameters [24]. In order to understand the roughening of the Si(001) surface during growth it would be important to know if step bunching and meandering can arise simultaneously. So far, no conclusive experimental evidence for the presence of the Schwoebel effect leading to meandering instability has been established.

In this Letter, we show that the difference in step stiffness and diffusion anisotropy induce a meandering instability which can account for the complex step structures observed in Si(001) epitaxial growth. We first present the linear two-dimensional stability analysis of a train of steps using a simplified extension of the model studied in reference [24]. We show that the interplay between diffusion anisotropy and the step stiffness effect under growth conditions induces a finite wavelength instability which is maximum for the in-phase modes. We present the stability phase diagram in the parameters space. Our results are complemented by a weak nonlinear analysis of the step meander which reveals a coarsening dynamics. Using a simple similarity argument, we show that the characteristic coarsening exponent is 1/2 and that the general solution of the CKS equations can be thought as a superposition of parabolas. Finally we conclude this Letter by discussing the possible relevance of our model to the experiment on Si growth and the consequences of the simultaneous existence of bunching and meandering instabilities.

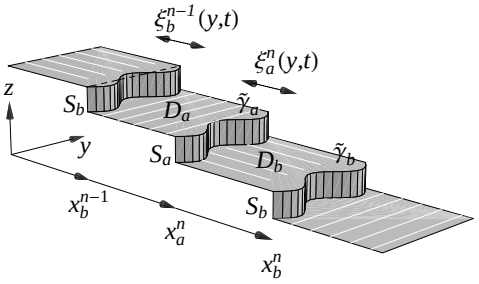

FIG. 1: Sketch of the Si(001) vicinal surface showing the alternation of terraces and steps S_a and S_b. Lines on terraces indicate the privileged diffusion directions. D_a, D_b and $\tilde{\gamma}_a$, $\tilde{\gamma}_b$ are the surface diffusion and step stiffness coefficients, respectively; x_a^n, x_b^n and $\xi_a^n(y,t)$, $\xi_b^n(y,t)$ are step positions and the corresponding perturbations.

The Si(001) vicinal surface consists of a periodic sequence of terraces where rows of 2×1 dimerized adatoms (terrace of type a) alternate with 1×2 dimerized adatoms (terrace of type b), as shown in Fig. 1 where we also in-

troduce several notations. On the reconstructed surface adatoms diffuse preferentially along dimer rows, giving rise to an anisotropic diffusion. Therefore, the steps separating the terraces are of two kinds. The S_a steps are rather straight while the S_b ones are very corrugated [25]. We shall allow each step to have a different step stiffness coefficient $\tilde{\gamma}_a$ and $\tilde{\gamma}_b$ [26]. For simplicity we neglect elastic interactions between steps and assume that the desorption of adatoms is negligible; we also neglect Erlich-Schwoebel effects. Let us denote by $x_a^n(y,t)$ and $x_b^n(y,t)$ the positions at time t of steps S_a and S_b respectively (cf. Fig. 1). During growth, the adatom concentrations on each terrace $C_a^n(x,y,t)$ and $C_b^n(x,y,t)$, obey the following diffusion equations [27]:

$$D_a\partial_x^2 C_a^n + D_b\partial_y^2 C_a^n = -F\,, \tag{1}$$
$$D_b\partial_x^2 C_b^n + D_a\partial_y^2 C_b^n = -F\,, \tag{2}$$

where D_a and D_b are the diffusion coefficients, and F the deposition flux. C_a^n and C_b^n are the difference of adatoms concentrations with respect to the uniform equilibrium concentration C_0 (taken to be the same on both terrace types). We assume for C_a^n and C_b^n, the following boundary conditions:

$$C_a^n(x_b^{n-1}) = C_{eq,b}^{n-1} \quad , \qquad C_a^n(x_a^n) = C_{eq,a}^n\,, \tag{3}$$
$$C_b^n(x_a^n) = C_{eq,a}^n \quad , \qquad C_b^n(x_b^n) = C_{eq,b}^n\,, \tag{4}$$

which correspond to instantaneous attachment kinetics, and can be considered as the simplest ones capturing the main physical effects (no diffusion along steps and negligible transparency). The adatom equilibrium concentrations $C_{eq,a}^n$ and $C_{eq,b}^n$ depend on the step curvatures κ_a^n and κ_b^n [12]:

$$C_{eq,a}^n = C_0\Gamma_a\kappa_a^n\,, \quad C_{eq,b}^n = C_0\Gamma_b\kappa_b^n\,, \tag{5}$$

with $\Gamma_b = \Omega\tilde{\gamma}_b/k_BT$ and $\Gamma_a = \Omega\tilde{\gamma}_a/k_BT$ (Ω is the unit atomic surface, T the temperature, and k_B the Boltzmann constant). The normal velocities of each step are $v_a^n = \dot{x}_a^n/(1+(\partial_y x_a^n)^2)^{1/2}$ and $v_b^n = \dot{x}_b^n/(1+(\partial_y x_b^n)^2)^{1/2}$, where

$$\dot{x}_a^n = \Omega\ [(D_b\partial_x C_b^n - D_a(\partial_y x_a^n)\partial_y C_b^n) - (D_a\partial_x C_a^n - D_b(\partial_y x_a^n)\partial_y C_a^n)]_{x=x_a^n}\,, \tag{6}$$
$$\dot{x}_b^n = \Omega\ [(D_a\partial_x C_a^{n+1} - D_b(\partial_y x_b^n)\partial_y C_a^{n+1}) - (D_b\,\partial_x C_b^n - D_a(\partial_y x_b^n)\partial_y C_b^n)]_{x=x_b^n}\,. \tag{7}$$

In order to get a nondimensional version of equations (1)-(7), we set the unit of length to be the initial size of the terrace l_0 and the unit of time $l_0^3/(C_0\Gamma_a\Omega D_a)$. The system is controlled by three independent positive nondimensional parameters:

$$f_0 = \frac{Fl_0^3}{C_0\Gamma_a D_a}\,, \quad \alpha_0 = \frac{D_b}{D_a}\,, \quad \delta_0 = \frac{\Gamma_a - \Gamma_b}{\Gamma_a}\,, \tag{8}$$

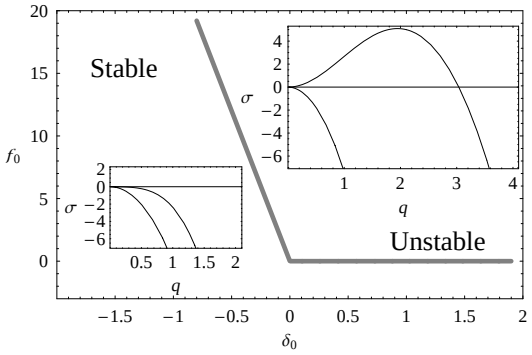

FIG. 2: Stability diagram in the plane (f_0, δ_0), for $\alpha_0 > 1$. The thick gray line $f_0 = f_{0c}$ given by Eq. (9), separates the unstable region (right side), from the stable one (left side). The dispersion relation $\sigma(q)$ with its two branches is shown in each region.

which respectively relate to the flux, diffusion anisotropy and step stiffness difference.

We investigate now the linear stability of a train of equidistant steps traveling at a constant velocity f_0 when perturbed transversally. The shape of the steps can be decomposed in Fourier modes of the form $x_a^n(y,t) = f_0t + 2n + \xi_a^n(y,t)$ and $x_b^n(y,t) = f_0t + 2n + 1 + \xi_b^n(y,t)$ with ξ_a^n and ξ_b^n the perturbation amplitudes varying as $\exp(\sigma(q,\phi)t + iqy + in\phi)$, where q is the wavenumber and ϕ the phase (see Fig. 1). Inserting these expressions into (1)-(7), we obtain the general dispersion relation $\sigma = \sigma(q,\phi)$. The dispersion relation possesses, for each ϕ, two branches corresponding to a stable σ_s and an unstable σ_u mode. The maximum growth rate is reached for the in-phase perturbation $\phi = 0$ (Fig. 2). In the following we consider only this in-phase mode, thus neglecting the n dependence $\xi_a^n = \xi_a$, and $\xi_b^n = \xi_b$ (the system is periodic in the x-direction with period $2l_0$). We find that the instability appears above a flux threshold f_{0c} given by,

$$f_0 > f_{0c} = -12\alpha_0\delta_0/(\alpha_0 - 1)\,, \tag{9}$$

where $f_0 > 0$. The stability domain in the plan (f_0, δ_0) is shown in Fig. 2. Typically the instability is related to a large diffusion D_b on terrace b ($\alpha_0 \gg 1$) accompanied by a small stiffness $\tilde{\gamma}_b$ of step S_b ($\delta_0 > 0$). Although the full expression of the dispersion relation is cumbersome, near the instability threshold we can introduce a small parameter ϵ measuring the distance to the threshold. This parameter arises naturally when considering the long wavelength limit, in which $q \to \epsilon q$. In this limit the relevant scaled parameters are chosen to be: $f_0 = \epsilon f$, $\delta_0 = \epsilon\delta$, $\alpha_0 = 1 + \epsilon^2\alpha$, together with a rescaling of the stiffness $\Gamma_a \to \epsilon^2\Gamma_a$. This scaling will lead to a consistent weak nonlinear expansion, as it will be shown below. To lowest order the two branches of $\sigma = \sigma(q,\phi)$

are,

$$\sigma_s = -4\epsilon^4 q^2 \,, \tag{10}$$

$$\sigma_u = \frac{\epsilon^6}{48} f\alpha(f\alpha + 12\delta)q^2 - \epsilon^6 q^4 \,. \tag{11}$$

The growth rate σ_u is maximum for the wavenumber $q_m = [f\alpha(f\alpha + 12\delta)]^{1/2}/4\sqrt{6}$. Even for vanishing δ (no difference between step stiffness) an instability is still present driven by diffusion anisotropy and growth effect, $\sigma_u(q_m) \sim f^4\alpha^4$. The physical mechanism of the instability is the point effect, increasing the diffusion around the maxima, combined with the anisotropy in diffusion between two consecutive terraces, locally impeding the compensation of the currents leaving and reaching the steps. If the anisotropy was absent, a simple difference in diffusion coefficients would not lead to an instability as a consequence of mass conservation.

Taking for example typical values for Si(001) at two different temperatures $T = 1000\,\mathrm{K}$ and $T = 800\,\mathrm{K}$ (with $l_0 = 2\,10^{-8}\,\mathrm{m}$ and $F = 0.1\,\mathrm{ML\,s^{-1}}$), $f_0 = 0.3$, and 4.3, $\alpha_0 = 45$, and 119, and $\delta_0 = 0.9$, we obtain that the typical wavelength of the meanders is of the order of 250 nm and 60 nm, respectively. These sizes are in the range of the transverse modulations (ripples) of the step bunches observed in the experiments [20–23].

We study at present the nonlinear evolution of the meandering instability, in the limit of weak amplitudes and long wavelengths. An inspection of Eqs. (10)-(11) for the damping and growth rates, suggests that we should consider different time scales and amplitudes for the stable and unstable branches. We introduce the functions $s(y,t)$ and $u(y,t)$ corresponding to the amplitudes of the stable and the unstable branches respectively. These amplitudes are related to the step shape by,

$$\begin{pmatrix} \xi_a \\ \xi_b \end{pmatrix} = \epsilon \mathcal{M}_0(\epsilon) \begin{pmatrix} \epsilon\, s \\ u \end{pmatrix} \,, \tag{12}$$

where $\mathcal{M}_0$ is the matrix formed with the eigenvectors associated to the linear dispersion relation and depends on the physical parameters $(f_0, \alpha_0, \delta_0)$. In order to obtain the relevant nonlinear dynamics we use a standard multiscale method. Adatoms concentrations and step shapes are expanded in powers of ϵ. The amplitudes of this expansion depend on the slowly varying space ϵy and two time variables $\epsilon^4 t$ and $\epsilon^6 t$. In particular the stable and unstable shape functions are given by $s = s(\epsilon^4 t, \epsilon y)$ and $u = u(\epsilon^6 t, \epsilon y)$. Solving diffusion equations (1-2) and boundary conditions (3-4) up to order ϵ^7, and inserting the results into the step velocity equations (6-7) we find the equation for the unstable mode:

$$\partial_t u = -\partial_y^2 \left[\frac{f\alpha}{48}(f\alpha + 12\delta)u + \partial_y^2 u + \frac{f}{12}(\partial_y u)^2 \right] \,, \tag{13}$$

where we renamed the slow variables $\epsilon^6 t \to t$ and $\epsilon y \to y$. After rescaling we can write Eq. (13) in the form

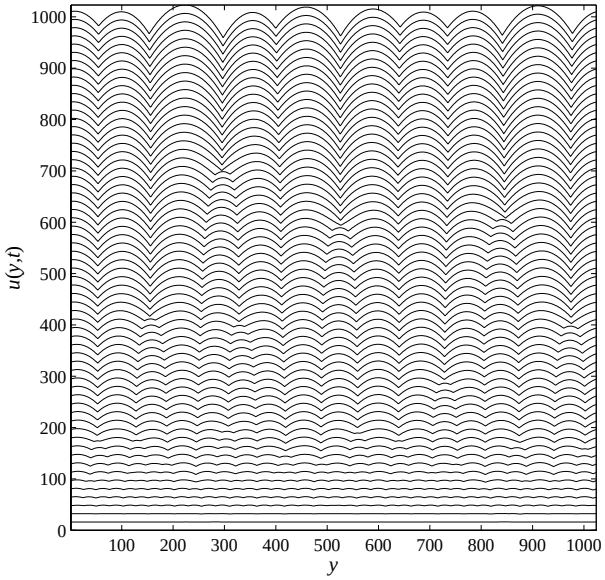

FIG. 3: Spacetime plot of $u(y,t)$ with nondimensional y and t axes, given by the numerical solution of the CKS equation. The coarse-graining of structures leads to a superposition of parabolas, with a size $\langle u^2\rangle^{1/2} \sim t$. In the long time state all the parabolas tend to have unity curvature at their maximum, and width increasing as $\sqrt{t}$.

$\partial_t u = -\partial_y^2[u + \partial_y^2 u + (\partial_y u)^2/2]$. This is a conserved version of the Kuramoto-Sivashinsky equation (CKS). The numerical simulations [28] of a related equation describing bunches created by an electromigration current, thus having an extra symmetry breaking term in $\partial_y^3 u$, have revealed a non interrupted coarsening dynamics with a characteristic size of coalesced step bunches increasing as $t^{1/2}$. In our context this $\partial_y^3 u$ term, leading to a dispersive drift, must be absent. Our direct simulations confirmed a $t^{1/2}$ scaling and also demonstrate a linear time growth of the characteristic meander amplitude $\langle u^2\rangle^{1/2} \sim t$ (spatial average is denoted $\langle \cdots \rangle$). A typical spatiotemporal evolution from a random initial condition is shown in Fig. 3. In the context of Bales-Zangwill meandering instability, it was shown that the dynamics of steps is fully nonlinear, excluding CKS equation, although it would be compatible with the basic symmetries of the system [15].

Simple similarity and matching arguments lead to a complete picture for the long time behavior of (13). It is worth noting that the CKS equation admits an exact particular solution in the form of a stationary parabola $u(y,t) = -y^2/2$. We also note that, for rapidly decreasing or bounded functions, the moment of order one of $u(y,t)$ is conserved while the second order moment satisfies

$$\frac{d}{dt}\frac{1}{2}\int u^2 dy = \int [(\partial_y u)^2 - (\partial_y^2 u)^2] dy \,, \tag{14}$$

showing that the amplitude of u tends to increase in regions where the gradient term $\partial_y u$ inside the integral

dominates the curvature term $\partial_y^2 u$. This suggests that the dynamics of large amplitude smooth regions of $u(y,t)$ is almost independent of the four derivative (stabilizing) term in (13). Trying a similarity solution

$$u = t^a \varphi(y/t^b)\,, \quad Y = y/t^b \tag{15}$$

of $\partial_t u = -\partial_y^2[u + (\partial_y u)^2/2]$, we find immediately the exponents $b = 1/2$ and $a = 1$, which agree with our numerical results. The fourth order derivative term behaves as $\partial_y^4 u \sim \partial_Y^4 \varphi/t$, which is consistent with the above assumption that it should be negligible in the considered regime. Moreover, the similarity equation for φ: $\varphi - (Y/2)\partial_Y \varphi + \partial_Y^2[\varphi + (\partial_Y \varphi)^2/2] = 0$ has a solution in the form of a bounded parabola:

$$u(y,t) = -y^2/2, \quad |y| < y_0(t) \tag{16}$$

and zero elsewhere. The parabola edge $y_0(t)$ is determined by the condition

$$\frac{d}{dt}\frac{1}{4}\int_0^{y_0(t)} y^4 dy = 2\int_0^{y_0(t)} y^2 dy\,, \tag{17}$$

a consequence of (14), which gives $y_0(t) = (16t/3)^{1/2}$. The general, asymptotic solution of (13) can be thought as a superposition of parabolas satisfying (16) (see Fig. 3). The joining region between the parabolas possesses a high curvature and can be described by the reduced inner equation $\partial_y^2 u(y) + (1/2)(\partial_y u(y))^2 = 2k^2 = \text{const.}$, whose solution is of the form $u(y) = 2\log[\cosh k(y - y_0(t))]$. Matching with the outer solution (16) we find that $k = y_0(t)/2 \sim \sqrt{t}$. Therefore, the curvature of the joining line increases as $\kappa \sim t$.

In this Letter, we have shown that the effect of step stiffness difference and diffusion anisotropy induces a meandering instability during surface growth. We have first presented a linear stability analysis of a train of steps using a simplified two-dimensional extension of the model studied in Ref. [24]. We have shown that the interplay between diffusion anisotropy and the step stiffness effect under growth conditions leads to a finite wavelength instability which is maximum for the in-phase mode. Our results are complemented by a weak nonlinear analysis of the step dynamics which reveals that the amplitude of the meanders is governed by the conserved Kuramoto-Sivashinsky equation (CKS) which displays non-interrupted coarsening. We believe that the morphology observed in experiments of molecular beam epitaxy on Si(001) slightly disoriented towards the [110] direction, reported in Refs. [20–23], can be explained by the nonlinear evolution of the step bunching and step meandering instabilities arising simultaneously. Indeed, we will present elsewhere an investigation of the two-dimensional dynamics originated by the nonlinear coupling between these kinetic effects, and we will discuss their role in the formation of the ripples shown for instance in Fig. 1 of Ref. [21].

We would like to thank J.-N. Aqua, I. Berbézier, M. Dufay, P. Politi, and C. Misbah for stimulating discussions.

* Electronic address: frisch@irphe.univ-mrs.fr
† Electronic address: Alberto.Verga@irphe.univ-mrs.fr

[1] J. Stangl, V. Holy, and G. Bauer, Rev. Mod. Phys. **76**, 725 (2004).
[2] A. Pimpinelli and J. Villain, *Physics of Crystal Growth* (Cambdrige University Press, 1998).
[3] Y. Saito, *Statistical Physics of Crystal Growth* (World Scientific, 1998).
[4] N. Néel, T. Maroutian, L. Douillard, and H.-J. Ernst, Phys. Rev. Lett. **91**, 226103 (2003).
[5] F. Nita and A. Pimpinelli, Phy. Rev. Lett. **95**, 106104 (2005).
[6] H.-C. Jeong and E. D. Williams, Surf. Sci. Rep. **34**, 171 (1999).
[7] P. Politi, G. Grenet, A. Marty, A. Ponchet, and J. Villain, Phys. Rep. **324**, 271 (2000).
[8] K. Yagi, H. Minoda, and M. Degawa, Surf. Sci. Rep. **43**, 45 (2001).
[9] V. A. Shchukin and D. Bimberg, Rev. Mod. Phys. **71**, 1125 (1999).
[10] K. Brunner, Rep. Prog. Phys. **65**, 27 (2002).
[11] G. S. Bales and A. Zangwill, Phys. Rev. B **41**, 5500 (1990).
[12] I. Bena, C. Misbah, and A. Valance, Phys. Rev. B. **47**, 7408 (1993).
[13] O. Pierre-Louis, C. Misbah, Y. Saito, J. Krug, and P. Politi, Phys. Rev. Lett. **80**, 4221 (1998).
[14] J. Kallunki and J. Krug, Phys. Rev. E **62**, 6229 (2000).
[15] F. Gillet, O. Pierre-Louis, and C. Misbah, Eur. Phys. J. B **18**, 519 (2000).
[16] G. Danker, O. Pierre-Louis, K. Kassner, and C. Misbah, Phys. Rev. E **68**, 020601 (2003).
[17] G. Danker, O. Pierre-Louis, K. Kassner, and C. Misbah, Phys. Rev. Lett. **93**, 185504 (2004).
[18] M. Sato, M. Uwaha, Y. Saito, and Y. Hirose, Phys. Rev. B. **67**, 125408 (2003).
[19] M. Sato, M. Uwaha, and Y. Saito, Phy. Rev. B **72**, 045401 (2005).
[20] C. Schelling, G. Springholz, and F. Schäffler, Phys. Rev. Lett. **83**, 995 (1999).
[21] C. Schelling, G. Springholz, and F. Schäffler, Thin Solid Films **369**, 1 (2000).
[22] A. M. Pascale, Ph.D. thesis, Marseille (2003).
[23] J. Mysliveček, C. Schelling, G. Springholz, F. Schäffler, B. Voigtländer, J. Krug, and P. Šmilauer, Surf. Sci. **520**, 193 (2002).
[24] T. Frisch and A. Verga, Phy. Rev. Lett. **94**, 226102 (2005).
[25] H. J. W. Zandvliet, Rev. Mod. Phys. **72**, 593 (2000).
[26] N. C. Bartelt and R. M. Tromp, Phys. Rev. B **54**, 11731 (1996).
[27] W. K. Burton, N. Cabrera, and F. C. Frank, Phil. Tans. Roy. Soc A **243**, 199 (1951).
[28] F. Gillet, Z. Csahok, and C. Misbah, Phys. Rev. B **63**, 241401 (2001).